

# Nanoparticle Enhancement Cascade for Sensitive Multiplex Measurements of Biomarkers in Complex Fluids with Surface Plasmon Resonance Imaging

Jan Hendriks,<sup>†</sup> Ivan Stojanovic,<sup>‡</sup> Richard B. M. Schasfoort,<sup>‡</sup> Daniël B. F. Saris,<sup>§,#</sup> and Marcel Karperien<sup>\*,†</sup>

<sup>†</sup>Department of Developmental BioEngineering, MIRA Institute for Biomedical Technology and Technical Medicine, University of Twente, Enschede, 7522 NB, The Netherlands

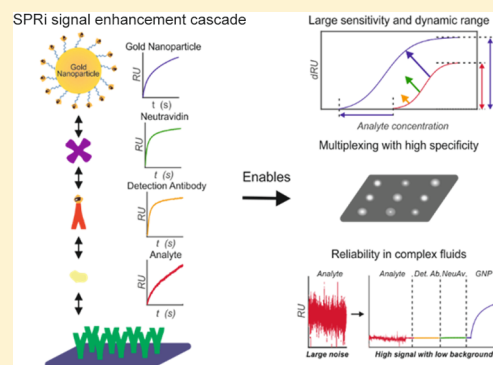
<sup>‡</sup>Medical Cell Biophysics, MIRA Institute for Biomedical Technology and Technical Medicine, University of Twente, Enschede, 7522 NB, The Netherlands

<sup>§</sup>Department of Orthopedics, UMC Utrecht, Utrecht, 3584 CX, The Netherlands

<sup>#</sup>Department of Reconstructive Medicine, MIRA Institute for Biomedical Technology and Technical Medicine, Faculty of Science and Technology, University of Twente, Enschede, 7522 NB, The Netherlands

## Supporting Information

**ABSTRACT:** There is a large unmet need for reliable biomarker measurement systems for clinical application. Such systems should meet challenging requirements for large scale use, including a large dynamic detection range, multiplexing capacity, and both high specificity and sensitivity. More importantly, these requirements need to apply to complex biological samples, which require extensive quality control. In this paper, we present the development of an enhancement detection cascade for surface plasmon resonance imaging (SPRi). The cascade applies an antibody sandwich assay, followed by neutravidin and a gold nanoparticle enhancement for quantitative biomarker measurements in small volumes of complex fluids. We present a feasibility study both in simple buffers and in spiked equine synovial fluid with four cytokines, IL-1 $\beta$ , IL-6, IFN- $\gamma$ , and TNF- $\alpha$ . Our enhancement cascade leads to an antibody dependent improvement in sensitivity up to 40 000 times, resulting in a limit of detection as low as 50 fg/mL and a dynamic detection range of more than 7 logs. Additionally, measurements at these low concentrations are highly reliable with intra- and interassay CVs between 2% and 20%. We subsequently showed this assay is suitable for multiplex measurements with good specificity and limited cross-reactivity. Moreover, we demonstrated robust detection of IL-6 and IL-1 $\beta$  in spiked undiluted equine synovial fluid with small variation compared to buffer controls. In addition, the availability of real time measurements provides extensive quality control opportunities, essential for clinical applications. Therefore, we consider this method is suitable for broad application in SPRi for multiplex biomarker detection in both research and clinical settings.



The complexity and multifactorial nature of chronic diseases requires the measurement of multiple biomarkers to provide robust information for both diagnosis and prognosis.<sup>1</sup> For this reason, there is a large interest in developing reliable biomarker detection systems suitable for clinical use. These systems should preferably combine high sensitivity, wide dynamic detection range, and multiplexing capacity in complex fluids with robust quality control opportunities. To our knowledge, considering the challenging demands, presently no system adequately meets these requirements.

Traditionally, biomarker measurements are performed using the ELISA format in both research and clinical settings. Although its benefits are clinically proven, the ELISA assay comes with a number of disadvantages: it requires relatively large sample volumes, has a small dynamic detection range necessitating the use of a dilution series, and has only limited

multiplexing capabilities. Furthermore, the need for expensive kits and bulky automation limits its usefulness for point-of-care applications.<sup>2</sup> Therefore, many alternative biomarker assays have been developed.<sup>3</sup> These can be separated into 2D planar assays and bead suspension assays. The 2D planar assays, such as Mesoscale Discovery and Searchlight, use a similar approach to the standard ELISA, with variation in the detection method (electro-chemiluminescent, chemiluminescent, fluorescent, or colorimetric). They apply a microarray format, allowing for multiplex measurements in small sample volumes. Despite the frequent use and the improvement over standard ELISAs, reports show a high interassay variability,<sup>4,5</sup> unreliability,<sup>4,6,7</sup> and lack of quality control opportunities.<sup>5,7</sup> Bead suspension

Received: January 17, 2018

Accepted: May 7, 2018

Published: May 7, 2018

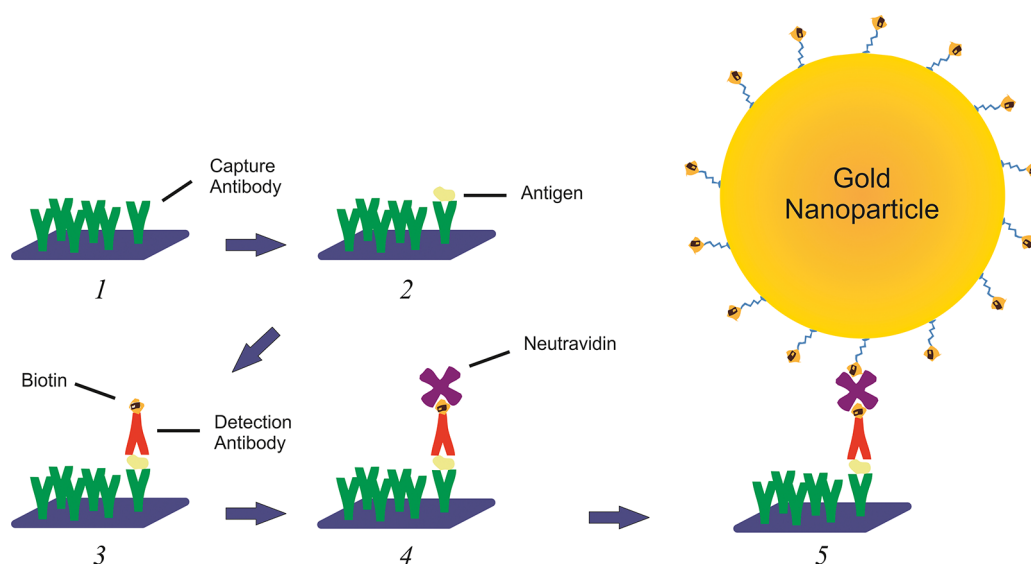


**Figure 1.** SPRI signal enhancement cascade using biotinylated gold nanoparticles. In this cascade, there is a sequential buildup of the complex and thus in SPRI signal. Initially, a specific capture antibody (1) interacts with the antigen (2); this is followed by a specific detection antibody toward that antigen in a sandwich format (3). Subsequently, neutravidin binds to the complex (4) followed by a commercially available biotinylated gold nanoparticle for large signal improvement (5).

assays are also often used for multiplex applications, especially in research settings. Of these, flow cytometry bead arrays and Luminex are the most common. These assays show excellent sensitivity over an acceptable dynamic detection range;<sup>8</sup> however, reports show a high interassay CV at low concentrations, resulting in unreliable results.<sup>9</sup> Also, the inherent increase in nonspecific interactions in suspension places a restraint on the multiplexing capacity.<sup>10</sup>

To overcome these limitations, new platforms are being developed that combine advanced surface chemistry and nanotechnology to create sophisticated sensing platforms.<sup>11</sup> In the literature, many elegant approaches are proposed that provide exceptional sensitivity,<sup>12</sup> an acceptable dynamic detection range,<sup>13</sup> and good multiplexing potential.<sup>14,15</sup> However, most of the aforementioned approaches are complex and are often end-point measurements. Due to the inherent variability in sensors and their “black box” nature, this leaves a large challenge for adequate and real-time quality control in clinical applications unaddressed.<sup>16</sup>

Surface plasmon resonance (SPR) is widely used in biomolecular interaction research applications for its sensitivity and real-time measurements. This technique evolved with SPR imaging (SPRI) to allow for simultaneous multiplex detection. More recently, its potential for biomarker detection has been explored. However, due to the small refractive index changes following interaction between a ligand and analyte, the signal-to-noise ratio is inadequate at low concentrations. Therefore, many attempts have been made to improve the sensitivity of measuring biomarkers. Natan's group was the first to show improved sensitivity using nanoparticle tags.<sup>17</sup> Following this, several approaches using various nanoparticles were explored for their suitability in taking low concentration measurements,<sup>18,19</sup> and more recently, the chemical conjugation of these nanoparticles was optimized.<sup>20</sup> However, little work has focused on the detection of biomarkers at high sensitivity and over a wide dynamic detection range in a multiplex setting. More particularly, ease of use and applicability in a future clinical setting is not often considered.

In this paper, we propose a method to improve both the sensitivity and the dynamic detection range in a multiplex setting with SPRI. We apply an antibody sandwich cascade using the biotin–neutravidin system in combination with commercially available biotinylated gold nanoparticles to sequentially increase the signal (schematically shown in Figure 1). We present a feasibility study both in clean buffers and in spiked equine synovial fluid with four cytokines, IL-1 $\beta$ , IL-6, IFN- $\gamma$ , and TNF- $\alpha$ . These cytokines are implicated in many diseases and can provide information on diagnosis and prognosis. However, they are present in pg/mL (low fM) in bodily fluids, therefore requiring high sensitivity. In addition, they can vary dramatically in concentration between disease states, requiring a large dynamic detection range.<sup>21</sup> We show that our method leads to a large improvement of both the sensitivity and the dynamic detection range and provides extensive quality control opportunities. Therefore, we feel that this approach is an important step forward for the broader application of the SPRI technique for multiplex biomarker detection. This can eventually lead to exciting applications in both research and clinical settings.

## EXPERIMENTAL SECTION

### Chemicals, Immunological Reagents, and Equipment.

Acetic acid, sodium acetate, phosphorous acid, phosphate buffered saline, magnesium chloride, Tween 20, Tween 80, and bovine serum albumin (BSA) were obtained from Sigma-Aldrich (Zwijndrecht, The Netherlands). The capture antibodies (cAb) and biotinylated detection antibodies (dAb) for IL-6 (cAb clone MQ2-13A5, dAb clone MQ2-39C3), IL-1 $\beta$  (cAb clone JK1B1, dAb clone JK1B2), and TNF- $\alpha$  (cAb clone Mab1, dAb clone Mab11), as well as the recombinant proteins IL-6, IL-1 $\beta$ , TNF- $\alpha$ , and IFN- $\gamma$  were purchased from Biologend (San Diego, USA). The capture antibodies and biotinylated detection antibodies for IFN- $\gamma$  (cAb clone A35, dAb clone B27) were obtained from Mybiosource (San Diego, USA). Neutravidin was obtained from Thermo Fisher (Waltham, USA). 40 nm biotinylated gold nanoparticles were purchased

from Cytodiagnostics (Burlington, Ontario, Canada). Preactivated sensors for amine coupling (G-type easy2spot) were purchased from Ssens bv (Hengelo, The Netherlands).

**Sensor Preparation.** Antibodies were immobilized on G-type easy2spot sensors via reaction to free amines using the Wasatch microfluidics continuous flow spotter (Wasatch Microfluidics, Salt Lake City, UT, US) for 30 min. Gel-type sensors were used for their increased binding capacity and more efficient use of the evanescent field, compared to a planar surface sensor. The immobilization reaction was performed in 50 mM acetic acid buffer (150  $\mu$ L per spot) with antibody concentrations specified in the respective experiments. An immobilization buffer of pH 4.6 provided antibody coupling with the highest retained activity and was therefore used for all experiments. At this pH, the antibodies are concentrated to the negatively charged hydrogel. Additionally, the low pH reduces the reactivity of lysines, leading to more directed coupling to primary amines. To reduce nonspecific interactions, the sensor was deactivated by 1% BSA in 50 mM acetate buffer at pH 4.6 for 7 min and subsequently with 0.2 M ethanolamine at pH 8.5 for an additional 7 min.

**SPRi Measurements.** The IBIS MX96 (IBIS Technologies, Enschede, The Netherlands) was used for the SPRi measurements. It applies an angle-scanning method with automatic fitting to determine SPR shifts. It has an automatic fluid-handling system and utilizes back-and-forth flow through a microfluidic flow cell that fits the array to enable minimal sample use. It is capable of measuring 96 spots simultaneously and is therefore highly suitable for our desired multiplex measurements. Measurements were programmed using SUIIT software (IBIS Technologies, Enschede, The Netherlands). In this program, the type of interaction, interaction times, samples, and regions of interest (ROIs) for the antibodies were set. Subsequently, a template was created and loaded into the IBIS data acquisition software. Before each experiment, an angle offset was applied to ensure a wide dynamic detection range. After programming, the machine provides automatic liquid handling and SPR angle measurements. For each experiment, 48 sensor spots were used. Back-and-forth flow was set to 10  $\mu$ L/min in a flow cell containing 12  $\mu$ L of sample. Sprint software was used for data collection and referencing. Data was subsequently exported to Matlab R2015a for further analysis and quality control through the use of custom scripts (available upon request).

**Antibody Affinity Measurements.** The affinity between the capture antibodies and cytokines was characterized by applying the kinetic titration method proposed by Schasfoort et al.<sup>22</sup> to avoid possible reduction in binding capacity under regeneration conditions. Sensors were prepared as explained above. Antibodies were spotted at 5, 2.5, 1.25, and 0.625  $\mu$ g/mL at eight spots per concentration leading to average RU of  $2000 \pm 250$ ,  $1500 \pm 225$ ,  $900 \pm 250$ , and  $300 \pm 50$ , respectively. Cytokines were dissolved in system buffer, containing PBS with 0.075% Tween 80, at a concentration of (1, 2, 4, 8, 16, 32, and 64 nM).

The kinetic titration was performed as follows: first, two blanks were injected followed by the respective cytokine at 1 nM and successive injections of two times increased concentrations up to 64 nM. The association time of each interaction was 10 min followed by a 12 min dissociation. Between each injection, the sensor was washed with system buffer.

Scrubber2 software was used to analyze the affinity data as described previously.<sup>22</sup> The blanks were subtracted, and the signal was zeroed to the first interaction. To determine the affinity of a specific spot, first the  $k_{\text{off}}$  rate was determined in the dissociation phase. Subsequently, the  $k_{\text{on}}$  rate was determined using a fixed  $k_{\text{off}}$  and a floating start point, to compensate for the titration setup. The affinity was determined for the antibodies at four spot densities leading to binding capacities ( $R_{\text{max}}$ ) and an affinity curve of  $K_{\text{D}}$  to  $R_{\text{max}}$ . The reported affinity for each antibody was calculated by extrapolating  $R_{\text{max}}$  to 100 (capture antibody affinities can be found in Figures S1–S4).

**SPRi Enhancement Cascade.** A SPRi signal enhancement cascade measurement was performed with the cytokines IL-6, IL-1 $\beta$ , TNF- $\alpha$ , and IFN- $\gamma$  in a broad dynamic detection range. Cytokine specific sensors were prepared as explained above. Antibodies were spotted at 5, 2.5, 1.25, 0.625, 0.3125, and 0.15625  $\mu$ g/mL with eight spots per concentration. Samples were dissolved in system buffer, containing PBS with 0.075% Tween 80 and 0.5% BSA. Cytokines were measured at a concentration ranging from 100 fg/mL ( $\sim$ 5 fM) to 1  $\mu$ g/mL ( $\sim$ 50 nM), spanning a dynamic detection range of 7 logarithms. A baseline of 5 min and an association time of 120 min were used. The detection antibody concentration was optimized for each cytokine, leading to 2.5  $\mu$ g/mL (16.5 nM) for IL-6, 5  $\mu$ g/mL (33 nM) for IL-1 $\beta$  and TNF- $\alpha$ , and 10  $\mu$ g/mL (66 nM) for IFN- $\gamma$ , respectively. Interaction with the detection antibody was performed with a baseline of 2 and 30 min association times. Neutravidin was used at a concentration of 1.5  $\mu$ g/mL (25 nM), 2 min baseline, and 15 min association (optimization shown in Figures S5 and S6), and the gold nanoparticle concentration was 77.69 mg/mL (0.2 nM), 2 min baseline, and 15 min association (optimization shown in Figure S7). After each cascade, the sensor was regenerated using a double regeneration pulse for 30s. Optimal regeneration conditions were antibody dependent and were determined according to the protocol adapted from Anderson et al.<sup>23</sup> The first regeneration pulse consisted of 200 mM phosphoric acid at pH 2.5, which was sufficient to remove IL-1 $\beta$ , TNF- $\alpha$ , and IFN- $\gamma$ . The second pulse consisted of 66 mM phosphoric acid, 333 mM MgCl<sub>2</sub> and 6.66 mM EDTA, and was required to regenerate IL-6 binding antibodies. Reproducibility of interaction after multiple regenerations is demonstrated in Figure S8.

The cascade interaction was performed as follows: First, a cytokine was injected, followed by a specific biotinylated detection antibody, neutravidin, and a biotinylated gold nanoparticle (40 nm diameter, which has optimal absorption vs scattering properties<sup>24</sup>). After each interaction, the sensor was washed to reduce the nonspecific signal. Each step in the cascade will increase the interaction signal proportionally and thus the sensitivity of the assay.

A typical experiment started with two full cascades with system buffer in each step to remove unbound antibody and to create a stable baseline. Subsequently, three blank cascades were measured, with system buffer in the cytokine interaction step, followed by the biotinylated detection antibody, neutravidin, and the biotinylated gold nanoparticle. These blanks were used to determine nonspecific interactions and provide the background correction. Finally, the cytokine cascades were performed starting from the lowest concentration.

Data was collected using Sprint software, referenced, and exported to Matlab. A custom Matlab script (available upon



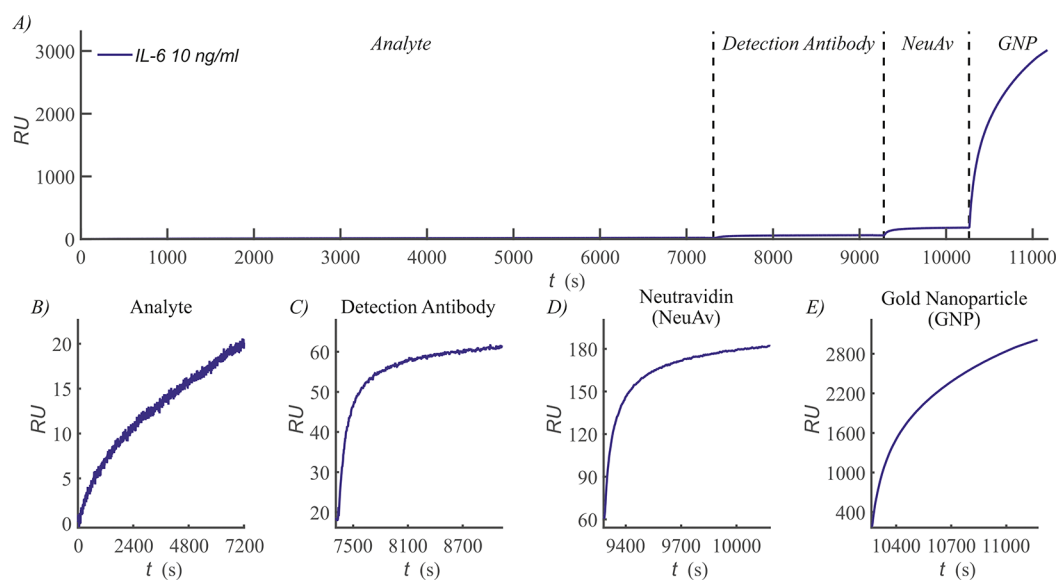


**Figure 2.** SPRi enhancement cascade response over time. The interaction with IL-6 is shown, followed by specific detection antibody, neutravidin, and gold nanoparticle. The graph (A) shows the average signal, in refractive index units (RU), combined from eight unique antibody spots with a uniform spotting density, corrected as described to  $R_{\max} = 100$  RU. The subplots (B–E) show the individual autoscaled graphs for each step in the signal enhancement cascade.

request) was used to determine the  $R_{\max}$  of each antibody spot, by 1–1 Langmuir fitting to at least three cytokine concentrations. Signals were extra- or interpolated to  $R_{\max}$  100 to correct for spotting irregularities. Subsequently, the signal from eight antibody spots of similar spotting density was combined to average the noise and to increase the robustness of signal. The limit of blank (LoB) and lower limit of detection (LLoD) were calculated as described by Armbruster and Pry<sup>25</sup> using the following equations:  $\text{LoB} = \text{mean}_{\text{blank}} + 1.645 (\text{SD}_{\text{blank}})$  and  $\text{LLoD} = \text{LoB} + 1.645 (\text{SD}_{\text{low concentration sample}})$ . The dynamic detection range was then calculated as the  $\log_{10}$  of the upper limit of detection (ULoD) divided by the LLoD.

**Multiplex Cytokine Measurement.** In the multiplex experiments, sensors with antibodies for IL-6, IL-1 $\beta$ , TNF- $\alpha$ , and IFN- $\gamma$  were spotted at a concentration of 5  $\mu\text{g}/\text{mL}$  with 10 spots per cytokine. As a control, 5  $\mu\text{g}/\text{mL}$  BSA was immobilized on eight spots. Samples were dissolved in system buffer, containing PBS with 0.075% Tween 80 and 0.5% BSA. Five mixtures of cytokines were measured. The first mixture contained the cytokines at a concentration in the lower region of the dynamic detection range determined previously. The concentrations chosen were 10, 33, 333, and 333 pg/mL for IL-6, IL-1 $\beta$ , TNF- $\alpha$ , and IFN- $\gamma$ , respectively. In mixtures 2 to 5, the concentration of a single cytokine was increased to a level higher in its dynamic detection range, while the other remained at the concentration of mixture 1. This leads to 333 pg/mL for IL-6 (mixture 2) and 1 ng/mL for IL-1 $\beta$  (mixture 3), TNF- $\alpha$  (mixture 4), and IFN- $\gamma$  (mixture 5). The detection antibodies were used in a mix in their optimal concentrations (2.5  $\mu\text{g}/\text{mL}$  (16.5 nM) for IL-6, 5  $\mu\text{g}/\text{mL}$  (33 nM) for IL-1 $\beta$  and TNF- $\alpha$ , and 10  $\mu\text{g}/\text{mL}$  (66 nM) for IFN- $\gamma$ , respectively). Neutravidin was used at a concentration of 1.5  $\mu\text{g}/\text{mL}$  (25 nM), and the gold nanoparticle concentration was 77.69 mg/mL (0.2 nM).

The multiplex experiment was performed as follows. Two cascades with system buffer were performed in each step to remove unbound antibody and to create a stable baseline. Next, three blank cascades were measured with system buffer in the cytokine interaction step, followed by the biotinylated detection

antibody mix, neutravidin, and the biotinylated gold nanoparticle. These blanks were used to determine nonspecific interactions and provide the background correction. Finally, the cytokine mixtures were measured starting from 1 to 5. At the end of the measurement, a calibration with 2% glycerol was performed.

In addition, we performed an experiment to determine the specificity of the capture and the detection antibodies. In this experiment, we used the same sensor as described in the standard multiplex experiment. Instead of mixtures, we injected single cytokines at 100 ng/mL with an association time of 120 min, followed by detection antibodies for 30 min. The detection antibodies were used in a mix in their optimal concentrations (2.5  $\mu\text{g}/\text{mL}$  (16.5 nM) for IL-6, 5  $\mu\text{g}/\text{mL}$  (33 nM) for IL-1 $\beta$  and TNF- $\alpha$ , and 10  $\mu\text{g}/\text{mL}$  (66 nM) for IFN- $\gamma$ , respectively). Neutravidin was used at a concentration of 1.5  $\mu\text{g}/\text{mL}$  (25 nM), and the gold nanoparticle concentration was 77.69 mg/mL (0.2 nM).

**Cytokine Measurement in Spiked Synovial Fluid.** To determine the feasibility of our approach with complex fluids, a spiking experiment was performed using equine synovial fluid. Sensors were prepared as explained above. A system buffer, containing 1 M NaCl, 2% Tween 20, and 0.5% BSA (adapted from ref 19), was used to reduce nonspecific binding. The detection antibody mix, containing optimal concentrations, neutravidin, and the gold nanoparticles were dissolved in this buffer. Cytokines were measured at a concentration at the higher end of their dynamic detection range, namely, 333 pg/mL for IL-6 and 1 ng/mL for IL-1 $\beta$ , respectively. They were dissolved in pure synovial fluid, half system buffer and half synovial fluid, or only system buffer as control.

The spiking experiment was performed as follows. Two cascades with system buffer in each step were performed to remove unbound antibody and to create a stable baseline. Subsequently, two blank cascades were measured with system buffer in the cytokine interaction step, followed by the biotinylated detection antibody mix, neutravidin, and the biotinylated gold nanoparticle. These blanks were used to

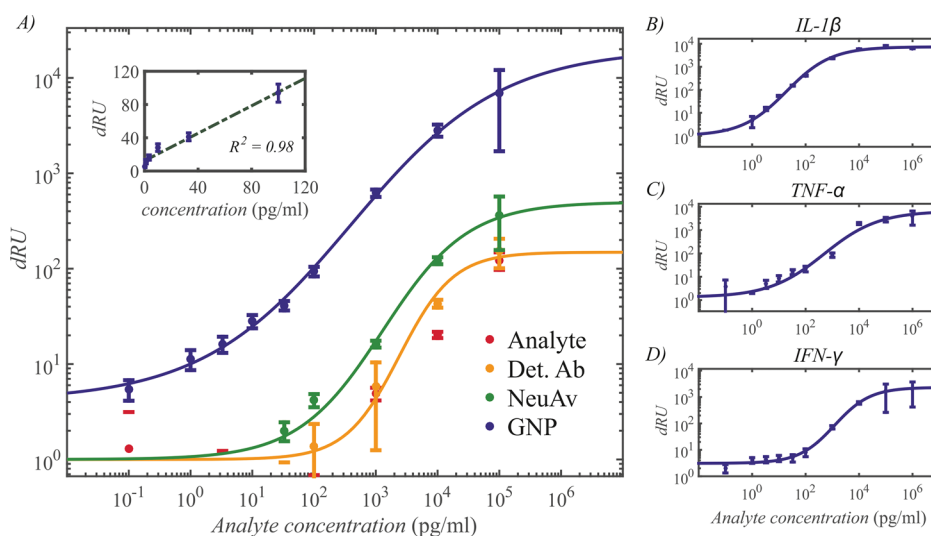


**Figure 3.** Enhancement cascade leads to sequential improvement in sensitivity and dynamic detection range. (A) The signal increase (dRU) after association with analyte, detection antibody (Det. Ab), neutravidin (NeuAv), and gold nanoparticle (GNP) is shown for IL-6 over a concentration range from 100 fg/mL to 100 ng/mL (1  $\mu$ g/mL is omitted due to clipping of too high signal). The inset shows the linear signal increase between 0.1 and 100 pg/mL ( $R^2 = 0.98$ ); data for other cytokines are shown in Figure S9. The signals represent the average of eight spots, corrected to  $R_{\max} = 100$  RU. Error bars depict standard deviations. Four-parameter logistic regression was used to fit the data points. (B–D) The signal after gold nanoparticle enhancement for IL-1 $\beta$ , IFN- $\gamma$ , and TNF- $\alpha$  over a concentration range from 100 fg/mL to 1  $\mu$ g/mL.

determine nonspecific interactions and provide the background correction. Then, alternating a blank and a spike in buffer, half synovial fluid or synovial fluid was measured. At the end of the measurement, a calibration with 2% glycerol was performed.

## RESULTS AND DISCUSSION

**SPRi Enhancement Cascade.** The signal enhancement of the SPRi measurement of cytokines using our sequential cascade is shown in Figure 2. Here, the response over time is shown after interaction with IL-6 at 10 ng/mL ( $\sim 500$  pM).

The graph shows association with IL-6 leads to a small signal of 20 RU. After the subsequent addition of biotinylated IL-6 antibody, this signal increases to 60 RU within 30 min. Association with neutravidin increases the signal further to 180 RU in 15 min. Finally, the biotinylated gold nanoparticle dramatically increases the signal to approximately 3000 RU. In combination, the three consecutive enhancement steps lead to a signal increase of 3, 9, and 150 times, respectively, compared to the IL-6 signal alone. Moreover, the use of a detection antibody increases not only the sensitivity but also the specificity for the respective cytokine leading to increased reliability of the measurement.

**Dynamic Detection Range Measurements.** The signal enhancement cascade was used to measure the cytokines IL-6, IL-1 $\beta$ , TNF- $\alpha$ , and IFN- $\gamma$  over a broad concentration range from 100 fg/mL ( $\sim 5$  fM) up to 1  $\mu$ g/mL ( $\sim 50$  nM) spanning a dynamic detection range of 7 logs. The resulting signal increase after each step in the enhancement cascade is shown in log–log plots in Figure 3.

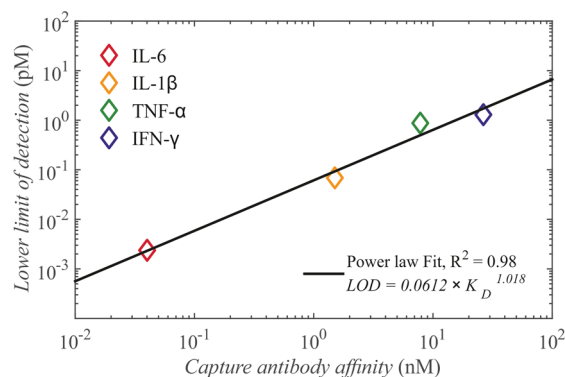
Figure 3A shows the signal increase after each enhancement step using IL-6 as the analyte. The lower limit of detection improves from 2 ng/mL after analyte association to 300 pg/mL after detection antibody, to 20 pg/mL after neutravidin, and finally to 50 fg/mL after the gold nanoparticle enhancement. This leads to an improvement in the limit of detection of 40 000 times. Additionally, the dynamic detection range increases from 3 logs to at least 7 logs. Moreover, the intra-assay precision is high (see Table S5 for more details),

especially in the linear range (CV < 10%) but also at low concentrations (CV < 20%). This allows for excellent concentration measurements, especially in the challenging lower portion of the dynamic detection range. We subsequently determined interassay precision (Table S6). This resulted in good precision at higher concentrations after analyte and antibody interaction and at lower concentration after neutravidin and gold nanoparticle interaction (CVs 2–20%). Thus, depending on the analyte concentration, one can select the best step in the amplification cascade for concentration measurement.

Figure 3B–D shows the signal increase over the dynamic detection range for IL-1 $\beta$ , IFN- $\gamma$ , and TNF- $\alpha$  after the gold nanoparticle signal enhancement. A similar increase in signal in each enhancement step was achieved as depicted with IL-6 (data shown over a range of spot densities in Figure S10). The figures show a good logistic regression fit and a broad dynamic detection range for the measured cytokines. Figure 4 shows a plot for the limit of detection versus the capture antibody affinity.

The data shows the detection limit and dynamic detection range are dependent on the individual cytokine and, thus, on the antibody pair used in the sandwich assay (more details in Table S7). This is shown by an increasing LOD of 1.2, 15, and 22 pg/mL for IL-1 $\beta$ , TNF- $\alpha$ , and IFN- $\gamma$ , respectively, compared to IL-6 and a decreasing dynamic detection range of 5 logs. This follows the trend in the affinity of the capture antibodies with a KD of 43 pM for IL-6, 1.5 nM for IL-1 $\beta$ , 7.8 nM for TNF- $\alpha$ , and 26.3 nM for IFN- $\gamma$ , respectively (affinity measurements are shown in Figures S1–S4). Although the affinities of the detection antibodies were not measured, the figure shows the capture antibody affinity is a good predictor for the sensitivity ( $R^2 = 0.98$ , Figure 4).

**Multiplex Cytokine Measurement.** The cytokines were measured in mixtures of both low and high concentrations to show the multiplexing potential of the enhancement cascade. The results are shown in Figure 5.



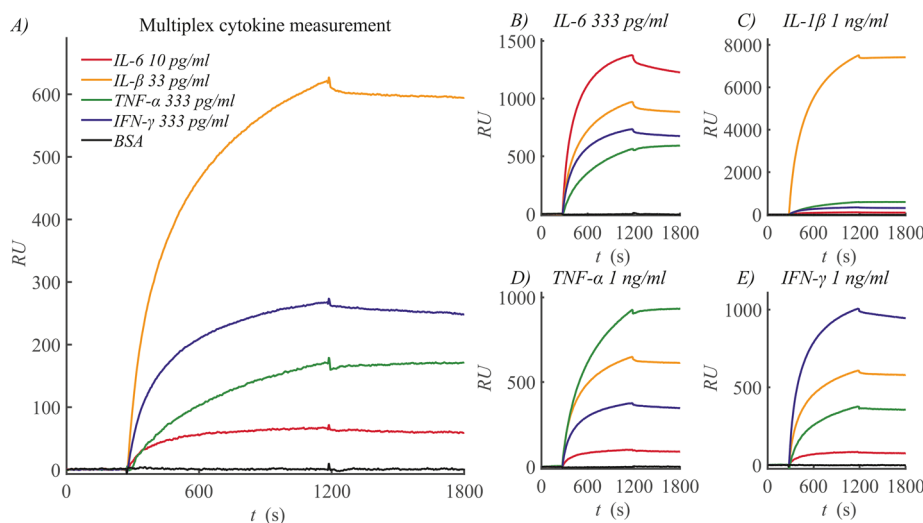
**Figure 4.** Lower limit of detection is plotted against the affinity of the capture antibody for the four cytokines measured. The figure shows good correlation between the capture antibody affinity and the LLOD in a power law function ( $R^2 = 0.98$ ). This indicates that the capture antibody affinity is the main predictor for the sensitivity of the assay. Variations in detection antibody affinity and biotin availability for neutravidin potentially play a less pronounced role.

Figure 5A shows the signal during the injection of the biotinylated gold nanoparticle as the last step in the signal enhancement cascade after incubation with a mixture of cytokines in the lower part of their respective dynamic detection range. The signals in the detection antibody and neutravidin steps were similar to those measured in earlier singleplex experiments at these concentrations, indicating specific interactions (data not shown). In Figure 5B–E, the concentration of one of the cytokines was increased by 3 times for IL-6 and IL-1 $\beta$  or 30 times for TNF- $\alpha$  and IFN- $\gamma$ , depending on the size of the dynamic detection range. As shown in Figure 5B–E, increasing the concentrations of individual cytokines leads to no (in the case of IL-6), minor (in the case of IL-1 $\beta$  and TNF- $\alpha$ ), or moderate (in the case of IFN- $\gamma$ ) nonspecific signal and to a large specific signal increase (further clarified in Figure S11). In Figure S12, the specificity is further assessed with injections of single cytokines and

detection antibodies. Here, we show there is very limited nonspecificity with both analyte and detection antibody. This indicates that the signal amplification method is suitable for multiplex measurements.

**Cytokine Measurement in Spiked Synovial Fluid.** For clinical biomarker assays, reliable measurements in complex fluids are essential. These complex fluids can range from serum to urine to synovial fluid, of which synovial fluid is considered the most challenging due to its high viscosity, particle contaminants, and limitations of small volumes. Here, we demonstrate a spike and recovery experiment of IL-6 and IL-1 $\beta$  in equine synovial fluid. The cytokines were spiked in synovial fluid, in synovial fluid diluted with buffer, or in pure buffer. In Figure 6, we show the results after gold nanoparticle association for IL-6 and IL-1 $\beta$ .

Figure 6 shows that direct measurements of cytokines in synovial fluid are impossible due to the large RU shifts caused by refractive index inhomogeneities in the synovial fluid. After incubation with synovial fluid, the sensor is washed and all subsequent measurement steps are performed in clean buffers resulting in stable baseline RUs allowing for reliable measurements (background signal shown in Figure S13). Consequently, after the enhancement cascade, both IL-6 and IL-1 $\beta$  can be measured in spiked diluted synovial fluid with no to very small variation compared to buffer controls (recovery of 98% and 89% for IL-6 and IL-1 $\beta$ , respectively). Considering the challenging nature of synovial fluid, this is excellent accuracy. In pure synovial fluid, the signal decreases to roughly half that of buffer controls but can still be readily measured with precision (recovery of 53% and 67% for IL-6 and IL-1 $\beta$ , respectively). The lower recovery in pure synovial fluid may be accounted for by its electrolyte composition which may influence the binding equilibrium. Together, this indicates that, while refractive index inhomogeneities in synovial fluid have an effect on the cytokine measurements, this effect is minimal in the enhancement cascade and can be easily corrected.



**Figure 5.** Cytokines were measured specifically in multiplex. (A) The RU signal during gold nanoparticle association after interaction with a mixture of cytokines in the lower region of the dynamic detection range, followed by the detection antibody and neutravidin cascade. The graph shows the baseline, followed by 15 min of association and 10 min of dissociation. The signals shown are an average of 10 spots. (B–E) Similar measurements as in (A) were performed; however, the concentration of a single cytokine is increased to the higher region in their dynamic detection range, without changing other concentrations in the mixture. In this way, the specificity and cross-reactivity of the cytokine detection was assessed.

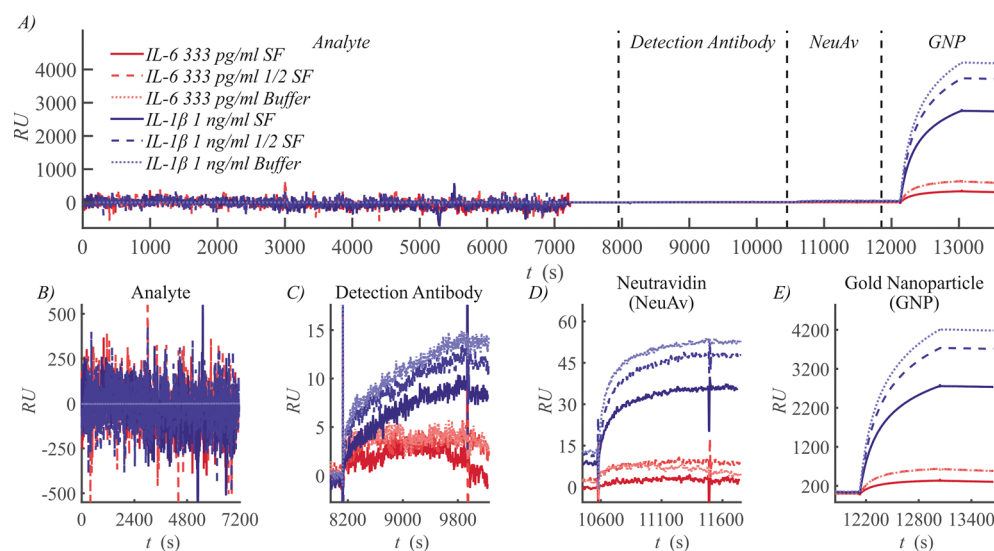


**Figure 6.** Spikes in synovial fluid can be measured with only minor variation compared to buffer controls. (A) The graph shows RU signal after interaction with a mixture of cytokines in the higher region of the dynamic detection range, followed by the detection antibody, neutravidin, and gold nanoparticle cascade. The cytokines were spiked in synovial fluid, in half synovial fluid and half buffer, or in pure buffer. The signals shown represent the average of 10 measurement spots. (B–E) Subplots are shown for each step in the enhancement cascade. The graphs show the baseline, followed by association and dissociation.

Biomarker detection systems for chronic diseases in both research and clinical settings require high sensitivity, wide dynamic detection range, and multiplexing capability in complex fluids with robust quality control opportunities. A system combining these demanding requirements does not yet exist.

In this study, we have implemented an enhancement cascade for SPRi that shows significant improvement in signal with only minor nonspecific background interactions. We have shown that the combination of the large signal increase with the reduction in standard deviation, through correction for ligand density variation, leads to very high sensitivity and a LLoD as low as 50 fg/mL (2 fM), depending on the capture antibody. Additionally, as the upper limit of detection is not reduced in the enhancement cascade, we obtained an extremely high dynamic detection range of 7 logarithms for quantitative measurements. This is comparable to, if not more sensitive than, the most sensitive commercial planar (Mesoscale discovery: average LLoD = 500 fg/mL, dynamic detection range = 3.5 logs) and bead suspension (Luminex: average LLoD = 2 pg/mL, dynamic detection range = 4 logs) assays available today.<sup>26</sup> When comparing our method to other experimental assays, we demonstrate similar (low fg/mL<sup>15,18</sup>) or better (low pg/mL<sup>13,19</sup>) sensitivity. Yet, our dynamic detection range is much wider than most reported, which is often no more than 3–4 logs.<sup>13,15,19</sup> This wide dynamic detection range is highly relevant considering the large difference between base level concentrations of different biomarkers and the large variation in individual biomarker concentrations between the healthy population and sick individuals but also between individual patients. Additionally, the large dynamic detection range can avoid the need for a dilution series. The sensitivity we have achieved is essential in the measurement of biomarkers, in particular for cytokines. The concentration of IL-6, TNF- $\alpha$ , and IFN- $\gamma$  is in the low pg/mL range in healthy subjects and will often not increase above 100 pg/mL in patients.<sup>27,28</sup> This already poses a large challenge in clinical diagnostics for these markers with nondetectable

values in a substantial subset of patients. For example, IL-1 $\beta$  is a highly interesting potent marker, associated with many inflammatory diseases, and could have diagnostic potential. However, its concentration in serum never exceeds 10 pg/mL, even in patients,<sup>29</sup> and can therefore not be reliably measured with most current clinical tools. The high sensitivity of our method does allow for measuring these challenging biomarkers, opening new opportunities for clinical diagnostics.

We have demonstrated the multiplexing potential of our method by specifically measuring the cytokines in mixtures compared to single controls. We show there is only minor cross-reactivity, especially with IL-6 and IL-1 $\beta$ . Moderate but larger cross reactivity was shown with TNF- $\alpha$  and IFN- $\gamma$ . Furthermore, we have demonstrated the potential of our method to measure biomarkers in complex fluids simultaneously in multiplex. To achieve this, we have used a single sensor to measure IL-6 and IL-1 $\beta$  spiked in equine synovial fluid, either pure or diluted with buffer. We have shown that only minor signal variations occur in half diluted synovial fluid compared to buffer controls. Considering the highly viscous nature of the synovial fluid with major impurities and the large nonspecific signal during the cytokine association phase, this represents remarkable accuracy. Association in pure synovial fluid leads to a small signal reduction of roughly half compared to that achieved in buffer controls. This reduction can potentially be attributed to the salt concentration, pH, and viscosity of the synovial fluid which can exert a specific effect on the antibodies and their binding characteristics. While this reduction might slightly decrease the sensitivity, it is probable that a small dilution in concentrated buffer can help diminish these effects. Therefore, we are confident that our method can be applied to measure simultaneously various cytokines sensitively and specifically in complex fluids.

The availability of real time measurements allows us to measure the signal at any given moment in the cascade. This provides extensive quality control opportunities, essential for clinical applications. For example, the evaluation of binding curves can provide more quantitative data and help detect and



eliminate nonspecific signals. In addition, it can provide actual binding capacities of spots allowing for a correction for spotting irregularities, which we have applied. As a result, we have achieved small intra-assay CVs with eight individual spots of no more than 10% in the linear range and less than 20% at the lowest concentrations, leading to excellent reproducibility. These are major advantages compared to standard assays, which show problems with spotting irregularities, assay reproducibility,<sup>30</sup> and large CVs in the low concentration range,<sup>31</sup> making them unsuitable for large scale clinical implementation.

Our enhancement cascade leads to excellent sensitivity and a dynamic detection range and works in multiplex, and we have shown feasibility for measuring in complex fluids. However, although our method works reliably for all cytokines tested, there is a large influence of the quality of the antibody pair on the outcome of the assay. For example, when comparing our best antibody pair (IL-6) to our worst (IFN- $\gamma$ ), the LLoD worsens from 50 fg/mL to 22 pg/mL, leading to an almost 1000 times lower sensitivity. In fact, we showed that there is a strong direct correlation between the affinity of the capture antibody and the sensitivity. Furthermore, we have shown larger nonspecific interactions in multiplex with our weakest antibody pairs. It is striking that the antibodies with the lowest affinity, highest limit of detection, and smallest dynamic detection range also show the highest cross-reactivity. This importance of the capture antibody is well-known and received extra attention due to the reproducibility crisis<sup>32</sup> but is still not often considered in detail. It is notoriously difficult to find high affinity antibody pairs<sup>33</sup> without ranking various antibodies from different suppliers, and specific information on antibody affinity is not known or is not given by suppliers.<sup>34</sup>

The SPRi technology specifically is well positioned to determine the antibody quality considering its long history in assessing molecular interactions. Therefore, this technique should be used to select good antibody pairs with high affinity and low cross-reactivity for clinical assay development. Considering our antibody panel, it becomes apparent that only the antibodies for IL-6 and IL-1 $\beta$  are suitable for clinical application. For the other cytokines, higher affinity antibody pairs should be found.

While the SPRi technology is highly suitable for multiplex measurements in small volumes and provides excellent quality control, it also has some limitations which are important to consider for large scale use. Signal fluctuations that occur with this technology require user experience and advanced software to deal with appropriately. In addition, the technology is still costly, with machines costing over 100k. This limits the availability of the technology. Smaller point of care devices that are under development could potentially address this issue.

We have demonstrated the feasibility of our enhancement cascade to measure biomarkers in multiplex in complex fluids. However, for clinical application, it is desired to further validate our method in human or equine samples. It is recommended to measure recovery and precision of spikes and potential interferences and to perform comparative measurements with standard methods in the field. This will be part of future work in which we will apply our method to measure cytokines in equine and human cohorts.

## CONCLUSION

In this paper, we present the development of an enhancement cascade for SPRi based on a sandwich assay and nanoparticle

amplification. This method not only can measure at high sensitivity and over a large dynamic detection range but also achieves this in multiplex, requiring small volumes, and still is very accurate even in synovial fluid, one of the most demanding complex bodily fluids. In addition, our method shows good reproducibility and allows for extensive quality control, essential for clinical application. In future work, we will further validate our method in equine and human patient cohorts to allow for both research and clinical diagnostic applications.

## ASSOCIATED CONTENT

### Supporting Information

The Supporting Information is available free of charge on the ACS Publications website at DOI: [10.1021/acs.analchem.8b00260](https://doi.org/10.1021/acs.analchem.8b00260).

Additional experiments, affinity measurements for the individual antibody–cytokine pairs, regeneration stability of the sensor, and precision of the assay (PDF)

## AUTHOR INFORMATION

### Corresponding Author

\*E-mail: [h.b.j.karperien@utwente.nl](mailto:h.b.j.karperien@utwente.nl). Phone: +31534893323.

### ORCID

Jan Hendriks: 0000-0002-3321-6866

### Author Contributions

All authors have given approval to the final version of the manuscript.

### Notes

The authors declare no competing financial interest.

## ACKNOWLEDGMENTS

We gratefully acknowledge the financial support by the Dutch Arthritis Foundation.

## REFERENCES

- (1) Frampton, J. P.; White, J. B.; Simon, A. B.; Tsuei, M.; Paczesny, S.; Takayama, S. *Sci. Rep.* **2015**, *4*, 4878.
- (2) Chikkaveeraiah, B. V.; Bhirde, A. A.; Morgan, N. Y.; Eden, H. S.; Chen, X. *ACS Nano* **2012**, *6*, 6546–6561.
- (3) Tighe, P. J.; Ryder, R. R.; Todd, I.; Fairclough, L. C. *Proteomics: Clin. Appl.* **2015**, *9*, 406–422.
- (4) Bastarache, J. A.; Koyama, T.; Wickersham, N. L.; Mitchell, D. B.; Mernaugh, R. L.; Ware, L. B. *J. Immunol. Methods* **2011**, *367*, 33–39.
- (5) Ellington, A. A.; Kullo, I. J.; Bailey, K. R.; Klee, G. G. *Clin. Chem.* **2010**, *56*, 186–193.
- (6) Backen, A. C.; Cummings, J.; Mitchell, C.; Jayson, G.; Ward, T. H.; Dive, C. *J. Immunol. Methods* **2009**, *342*, 106–114.
- (7) Cretich, M.; Damin, F.; Chiari, M. *Analyst* **2014**, *139*, 528–542.
- (8) Moncunill, G.; Aponte, J. J.; Nhabomba, A. J.; Dobaño, C. *PLoS One* **2013**, *8*, e52587.
- (9) Tighe, P.; Negm, O.; Todd, I.; Fairclough, L. *Methods* **2013**, *61*, 23–29.
- (10) Juncker, D.; Bergeron, S.; Laforte, V.; Li, H. *Curr. Opin. Chem. Biol.* **2014**, *18*, 29–37.
- (11) Lei, J.; Ju, H. *Chem. Soc. Rev.* **2012**, *41*, 2122–2134.
- (12) Munge, B. S.; Coffey, A. L.; Doucette, J. M.; Somba, B. K.; Malhotra, R.; Patel, V.; Gutkind, J. S.; Rusling, J. F. *Angew. Chem., Int. Ed.* **2011**, *50*, 7915–7918.
- (13) Jo, H.; Kim, S.-K.; Youn, H.; Lee, H.; Lee, K.; Jeong, J.; Mok, J.; Kim, S.-H.; Park, H.-S.; Ban, C. *Biosens. Bioelectron.* **2016**, *81*, 80–86.
- (14) Osterfeld, S. J.; Yu, H.; Gaster, R. S.; Caramuta, S.; Xu, L.; Han, S.-J.; Hall, D. A.; Wilson, R. J.; Sun, S.; White, R. L.; Davis, R. W.; Pourmand, N.; Wang, S. X. *Proc. Natl. Acad. Sci. U. S. A.* **2008**, *105*, 20637–20640.



- (15) Lai, G.; Wu, J.; Ju, H.; Yan, F. *Adv. Funct. Mater.* **2011**, *21*, 2938–2943.
- (16) Master, S. R.; Bierl, C.; Kricka, L. J. *Drug Discovery Today* **2006**, *11*, 1007–1011.
- (17) Lyon, L. A.; Musick, M. D.; Natan, M. J. *Anal. Chem.* **1998**, *70*, 5177–5183.
- (18) Krishnan, S.; Mani, V.; Wasalathanthri, D.; Kumar, C. V.; Rusling, J. F. *Angew. Chem., Int. Ed.* **2011**, *50*, 1175–1178.
- (19) Martinez-Perdiguero, J.; Retolaza, A.; Bujanda, L.; Merino, S. *Talanta* **2014**, *119*, 492–497.
- (20) Špringer, T.; Chadtová Song, X.; Ermini, M. L.; Lamačová, J.; Homola, J. *Anal. Bioanal. Chem.* **2017**, *409*, 4087–4097.
- (21) Dama, P.; Ledoux, D.; Nys, M.; Vrindts, Y.; De Groote, D.; Franchimont, P.; Lamy, M. *Ann. Surg.* **1992**, *215*, 356–362.
- (22) Schasfoort, R. B. M.; Andree, K. C.; van der Velde, N.; van der Kooi, A.; Stojanović, I.; Terstappen, L. W. M. M. *Anal. Biochem.* **2016**, *500*, 21–23.
- (23) Andersson, K.; Hämäläinen, M.; Malmqvist, M. *Anal. Chem.* **1999**, *71*, 2475–2481.
- (24) Zeng, S.; Yu, X.; Law, W.-C.; Zhang, Y.; Hu, R.; Dinh, X.-Q.; Ho, H.-P.; Yong, K.-T. *Sens. Actuators, B* **2013**, *176*, 1128–1133.
- (25) Armbruster, D. A.; Pry, T. *Clin. Biochem. Rev.* **2008**, *29*, S49–S52.
- (26) Fu, Q.; Zhu, J.; Van Eyk, J. E. *Clin. Chem.* **2010**, *56*, 314–318.
- (27) Chung, S.-J.; Kwon, Y.-J.; Park, M.-C.; Park, Y.-B.; Lee, S.-K. *Yonsei Med. J.* **2011**, *52*, 113–120.
- (28) Arican, O.; Aral, M.; Sasmaz, S.; Ciragil, P. *Mediators Inflammation* **2005**, *2005*, 273–279.
- (29) Di Iorio, A.; Ferrucci, L.; Sparvieri, E.; Cherubini, A.; Volpato, S.; Corsi, A.; Bonafè, M.; Franceschi, C.; Abate, G.; Paganelli, R. *Cytokine* **2003**, *22*, 198–205.
- (30) Berthoud, T. K.; Manaca, N. M.; Quelhas, D.; Aguilar, R.; Guinovart, C.; Puyol, L.; Barbosa, A.; Alonso, P. L.; Dobaño, C. *Malar. J.* **2011**, *10*, 115.
- (31) Chowdhury, F.; Williams, A.; Johnson, P. J. *Immunol. Methods* **2009**, *340*, 55–64.
- (32) Bake, M. *Nature* **2015**, *521*, 274–276.
- (33) Marx, V. *Nat. Methods* **2013**, *10*, 703–707.
- (34) Schonbrunn, A. *Mol. Endocrinol.* **2014**, *28*, 1403–1407.